



# A New Emission Mode of PSR B1859+07

Tao Wang<sup>1,2</sup> , P. F. Wang<sup>1,2,3</sup> , J. L. Han<sup>1,2,3</sup> , Yi Yan<sup>1,2</sup>, Ye-Zhao Yu<sup>4</sup>, and Feifei Kou<sup>5</sup>

<sup>1</sup> National Astronomical Observatories, Chinese Academy of Sciences, Beijing 100101, China; [pfwang@nao.cas.cn](mailto:pfwang@nao.cas.cn), [hjl@nao.cas.cn](mailto:hjl@nao.cas.cn)

<sup>2</sup> School of Astronomy and Space Science, University of Chinese Academy of Sciences, Beijing 100049, China

<sup>3</sup> The key Laboratory for Radio Astronomy and Technology, Chinese Academy of Sciences, Beijing 100101, China

<sup>4</sup> Qiannan Normal University for Nationalities, Duyun 558000, China

<sup>5</sup> Xinjiang Astronomical Observatories, Chinese Academy of Sciences, Urumqi 830011, China

Received 2023 April 26; revised 2023 May 6; accepted 2023 May 10; published 2023 September 13

## Abstract

Previous studies have identified two emission modes in PSR B1859+07: a normal mode that has three prominent components in the average profile, with the trailing one being the brightest, and an anomalous mode (i.e., the A mode) where emissions seem to be shifted to an earlier phase. Within the normal mode, further analysis has revealed the presence of two submodes, i.e., the cW mode and cB mode, where the central component can appear either weak or bright. As for the anomalous mode, a new bright component emerges in the advanced phase while the bright trailing component in the normal mode disappears. New observations of PSR B1859+07 using the Five-hundred-meter Aperture Spherical Radio Telescope (FAST) have revealed the existence of a previously unknown emission mode, dubbed the Af mode. In this mode, all emission components seen in the normal and anomalous modes are detected. Notably, the mean polarization profiles of both the A and Af modes exhibit a jump in the orthogonal polarization angle modes in the bright leading component. The polarization angles for the central component in the original normal mode follow two distinct orthogonal polarization modes in the A and Af modes respectively. The polarization angles for the trailing component show almost the same but a small systematic shift in the A and Af modes, roughly following the values for the cW and cB modes. Those polarization features of this newly detected emission mode imply that the anomalous mode A of PSR B1859+07 is not a result of “phase shift” or “swooshes” of normal components, but simply a result of the varying intensities of different profile components. Additionally, subpulse drifting has been detected in the leading component of the Af mode.

**Key words:** (stars:) pulsars: individual (PSR B1859+07) – polarization – plasmas

## 1. Introduction

Pulsars are highly magnetized, rotating neutron stars. The pulses of every period exhibit varying morphology and polarization. Pulse sequences manifest nulling, mode changing, and subpulse drifting phenomena. Rankin et al. (2006) found an unusual phenomenon that PSRs B0919+06 and B1859+07 occasionally manifest as a shift of emission toward early rotation phases, which was termed “swooshes” by Wahl et al. (2016) and Rajwade et al. (2021) or the “flare-state” by Perera et al. (2016). The “swooshes” of PSR B1859+07 last for about 20–120 periods, and happen gradually within several periods and somehow quasi-periodically about every 150 rotations (Wahl et al. 2016; Wang et al. 2022). In the normal state, PSR B1859+07 exhibits the bright and quiet modes (Rajwade et al. 2021; Wang et al. 2022), in which the central component is bright or weak respectively, which we term as two submodes, i.e., the central-weak mode “cW” and central-bright mode “cB”. The morphology, periodicity and possible physical origins of such a shift-like emission for PSR B0919+06 have also been investigated, e.g., by Han et al. (2016). These diverse

features provide valuable insight into the physical conditions and emission processes in the pulsar magnetosphere.

There have been a number of interpretations of the “swooshes” phenomenon. Based on the symmetry of pulse profiles and the cone–core beam model, Rankin et al. (2006) proposed that the “swooshes” are caused by partial illumination of the emission cone, which might originate from the emission processes or “absorption” (Bartel et al. 1981). Rajwade et al. (2021) argued that the “swooshes” result from the cutting of different parts of flux tubes due to the shrinking and expanding of the magnetosphere. Wahl et al. (2016) and Gong et al. (2018) attributed the “swooshes” to the possible orbital dynamics in a binary system. These diverse interpretations need to be further verified, and the real origin of “swooshes” remains to be uncovered.

In this paper, we report the detection of a new emission mode of PSR B1859+07 by using the Five-hundred-meter Aperture Spherical Radio Telescope (FAST, Nan 2006; Nan et al. 2011), which has a clear implication for the origin of “swooshes”. The paper is organized as follows. In Section 2, FAST observations and data reduction are briefly introduced.

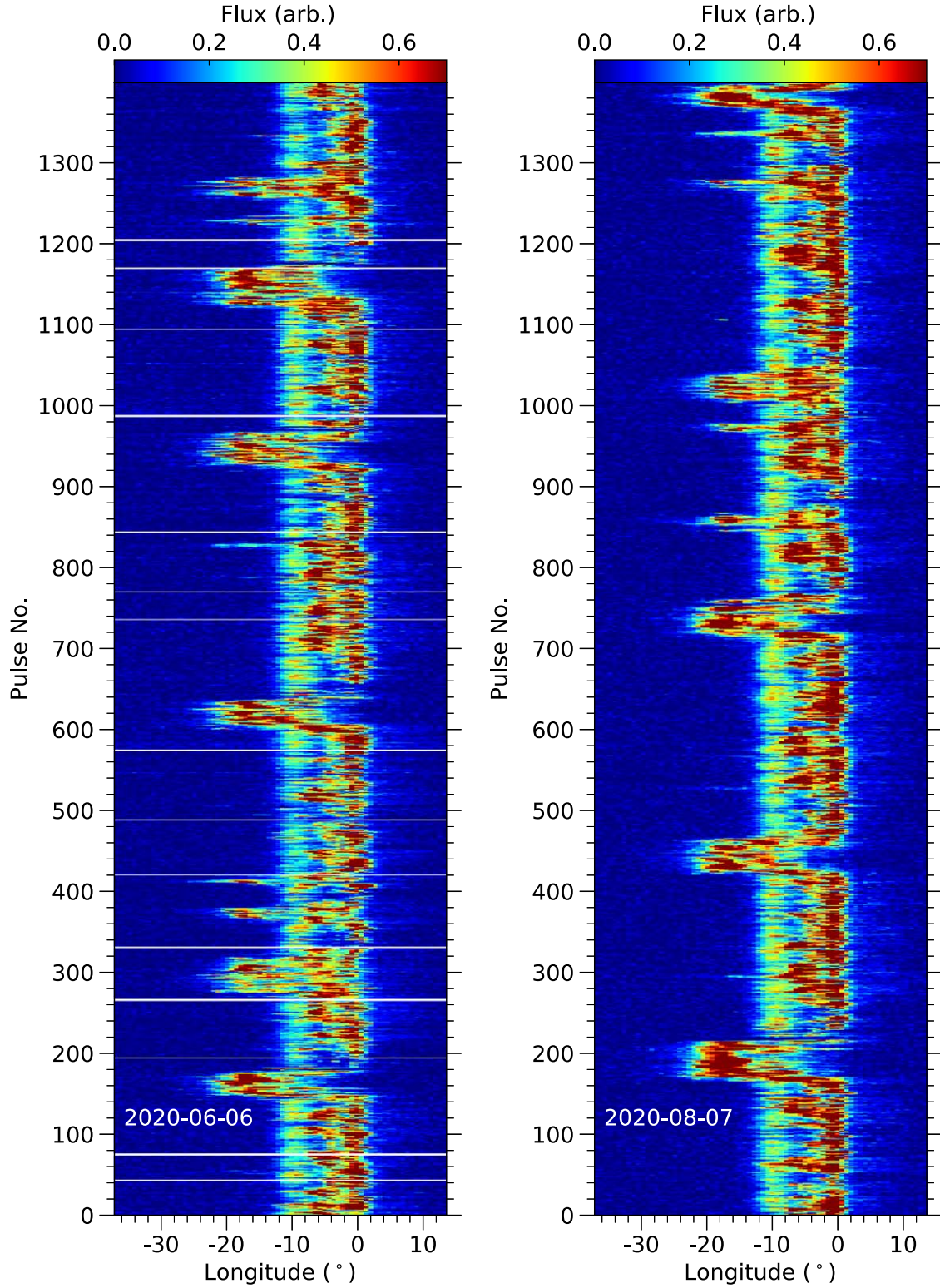


**Figure 1.** Pulse sequences of PSR B1859+07 obtained from two FAST observation sessions on 2020 June 6 (2020-06-06) and August 7 (2020-08-07) in the GPPS survey. Data with radio-frequency interference are eliminated as marked by white lines.

The results for the morphology, polarization behaviors and the subpulse drifting phenomenon are reported in Section 3. A summary and discussion are given in Section 4.

## 2. Observations and Data Reduction

We made two observations of PSR B1859+07 on 2020 June 6 (2020-06-06) and 2020 August 7 (2020-08-07) with the  $L$ -band 19-beam receiver of the FAST (Jiang et al. 2020), during the verification observations for the FAST Galactic Plane Pulsar Snapshot (GPPS) survey (Han et al. 2021). Each tracking observation lasts for 15 minutes. The data were recorded with full polarization, which has a central frequency of 1.25 GHz and a bandwidth of 500 MHz. The data for 2048 frequency channels are stored with a time resolution of 49.152  $\mu$ s. Details of observations can be found in Han et al. (2021). Before each observation session, two minutes of data are recorded from the receiver with calibration signals of 1 K on-off noise injected every 2 s, which are used for the correction of the bandpass of the receiver and also the calibration of the polarization performance of the receiver.

The special targeted FAST observations of PSR B1859+07 on 2019 December 03 (2019-12-03) and 2020 November 22 (2020-11-22) (Wang et al. 2022) are also included in this work for the verification of new results.

Offline data processing is as follows. We first dedispersed the data and formed single pulse sequences with the ephemeride by using DSPSR (van Straten & Bailes 2011). Radio-frequency interference was then removed for frequency channels and time by using PSRCHIEVE (Hotan et al. 2004). The pulses were finally calibrated in polarization with noise diodes, following the procedures presented by Wang et al. (2023).

## 3. Results

The pulse sequences are obtained from the two observation sessions in the GPPS survey on 2020-06-06 and 2020-08-07, as shown in Figure 1. The pulse sequences from special targeted FAST observations of PSR B1859+07 on 2019-12-03 and 2020-11-22 have been shown in Wang et al. (2022). Obviously different emission modes switch frequently with various durations. As previously observed (Rankin et al. 2006; Wahl et al. 2016; Rajwade et al. 2021), the normal emission mode has three prominent components in the averaged profile, and the trailing one is the brightest. According to the brightness of the central component, the normal emission mode can be further classified into two submodes: the “cB mode” with a bright central component, corresponding to the “B mode” in Wang et al. (2022) and Rajwade et al. (2021), and the “cW mode” with a weak central component, corresponding to the “Q mode” in Wang et al. (2022) or the “A mode” in Rajwade et al. (2021). The profile and polarization differences of these two modes have been studied in great detail by Wang et al. (2022)

**Table 1**  
Period Ranges for Anomalous Modes in Two Observation sessions of the FAST GPPS Survey

Period Range (No.–No.)	Type	Duration (periods)
2020-06-06		
153–172	A	19
275–315	Af	40
367–379	A	12
409–415	Af	16
494–495	Af	1
606–630	A	24
787–788	A	1
824–828	Af	4
930–955	A	25
955–965	Af	10
1120–1140	Af	20
1140–1167	A	27
1225–1229	A	4
1256–1281	Af	35
1332–1333	Af	1
2020-08-07		
170–216	A	46
294–296	A	2
425–455	A	30
455–465	Af	10
714–720	Af	6
720–742	A	22
742–760	Af	18
845–867	Af	22
968–977	Af	9
1006–1038	Af	32
1104–1106	Af	2
1268–1278	Af	10
1332–1338	Af	6
1367–1388	A	21
1388–1395	Af	7

and Rajwade et al. (2021). What we are concerned about in this paper is the “swooshes”, which exhibit a new bright component in the advanced phase range of  $-12^\circ$  to  $-28^\circ$ . The ranges of period for the anomalous modes are listed in Table 1.

### 3.1. The Anomalous-filled Mode: “Af Mode”

As shown in Figure 1, there are two types of “swooshes” revealed by the sensitive FAST observations. One is the conventional “swooshes” in which a new bright component emerges in the advanced phase range while the bright trailing component seen in the normal mode completely disappears as if the emission components are shifted to an earlier phase. We now label it as “mode A”. The other one is not such “swooshes” but appears as a new emission mode, dubbed the “Af mode”, which hosts all emission components seen from the normal mode and anomalous mode, though the leading component (almost the same one as in the anomalous



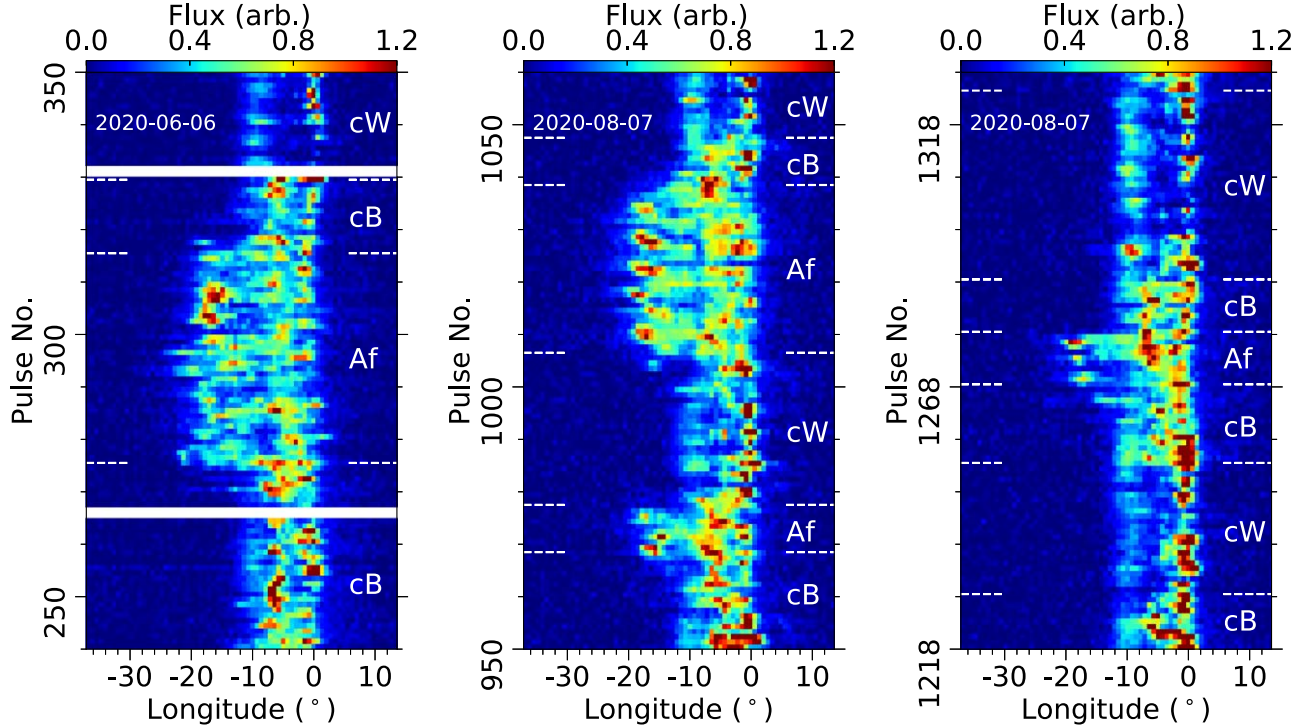


**Figure 2.** Examples of the Af mode, which not only show the new leading component in the A mode but also have slightly squashed components of the cB and cW modes. The different emission modes are marked for different segments of pulse sequences. The data with radio-frequency interference are eliminated as marked out by white lines.

“A mode”) and the trailing component (almost the same one as in the normal mode) shrink in the longitude phases. Examples of such an anomalous-filled mode, i.e., “the Af mode”, are shown in Figure 2.

We identify 30 anomalous emission events from our two FAST GPPS observation sessions in the GPPS survey, lasting for 1 to 46 rotations, including 12 events for the “A mode” and 18 events for the “Af mode”, as listed in Table 1. In fact, such an anomalous-filled mode has been noticed and shown in the FAST data of 2020-11-22 published by Wang et al. (2022), e.g., the pulses around period numbers: 450, 1270, 1580, 1990, 2140, 2700, 3170, 3510 and 4570 in their Figure 2, and the upper half of their Figure 6 give the best illustration, but this mode was not well investigated, especially its polarization properties. We also obtain results from previous FAST observation session of 2019-12-03 and found many segments for the Af mode.

### 3.2. Polarization Profiles for Different Modes

Polarization profiles of pulsars provide insights into the emission geometry in the pulsar magnetosphere. Comparing polarization profiles for different modes, especially the curves of polarization angle (PA), can aid in distinguishing between

“swooshes” in different longitudinal phases and different modes of pulsar emission.

By averaging the pulses in the different modes, we get the mean pulse polarization profiles for the two FAST GPPS observation sessions in Figure 3. The polarization profiles for the cW mode and the cB mode have been compared by Wang et al. (2022) already. We here compare the polarization profiles for two normal modes (cW and cB) with the two anomalous modes (A and Af). The profiles for all modes are consistent with each other in the two observations. When the two previous FAST observation sessions of PSR B1859+09 are considered, the slight profile difference between the four observations for the A mode and the Af mode reflects the unstable profiles caused by insufficient numbers of periods for the averaging process. Very striking are the PA curves for the Af mode, which are in the orthogonal mode of the PA in the A mode in the phase range between  $-8.5^\circ$  and  $-1.5^\circ$ . In general, the PA curves of the Af mode follow the curves of the cB and cW modes except for the phase range around  $0^\circ$ .

One may compare the polarization profiles by plotting them together as in Figure 4. The results for the fractional linear polarization and the fractional circular polarization are very consistent with each other on the two days. The fractional linear polarization of the “A mode” emission differs significantly from that of the normal modes and the Af mode with a

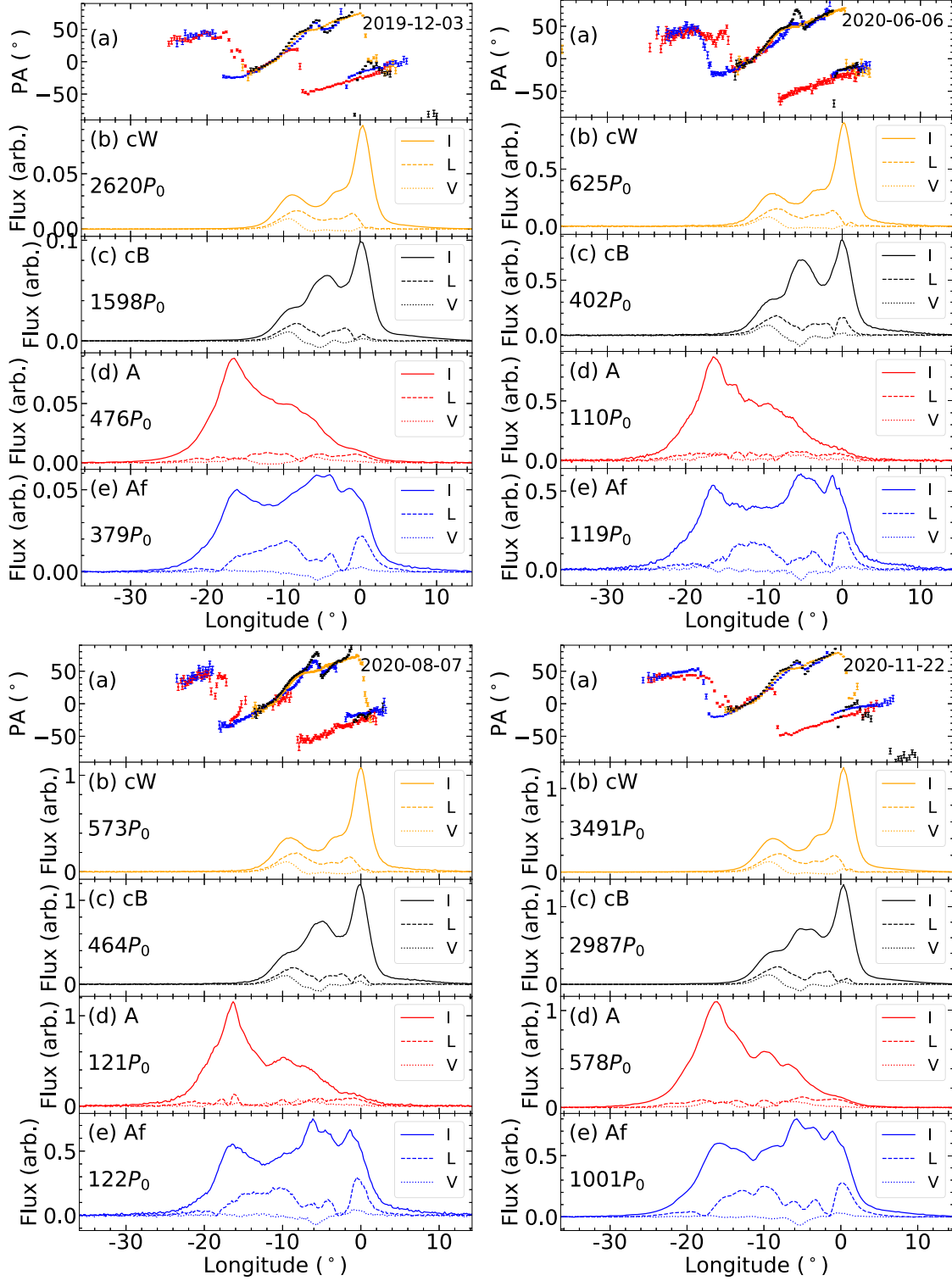


**Figure 3.** The mean pulse profiles of the emission modes: cW (orange), cB (black), A (red) and Af (blue) from four FAST observation sessions, with the number of pulsar periods marked in each subpanel for each mode. In general, profiles for the normal mode are consistent with each other in the four observations. The slight differences for the Af mode profiles are caused by insufficient number of periods for the averaging process. The PA curves in the Af mode are in the orthogonal mode of the A mode in the phase range  $[-8.5^\circ, -1.5^\circ]$ . The PA data are plotted only when linear polarization intensity exceeds five times the standard deviation of off-pulse data.

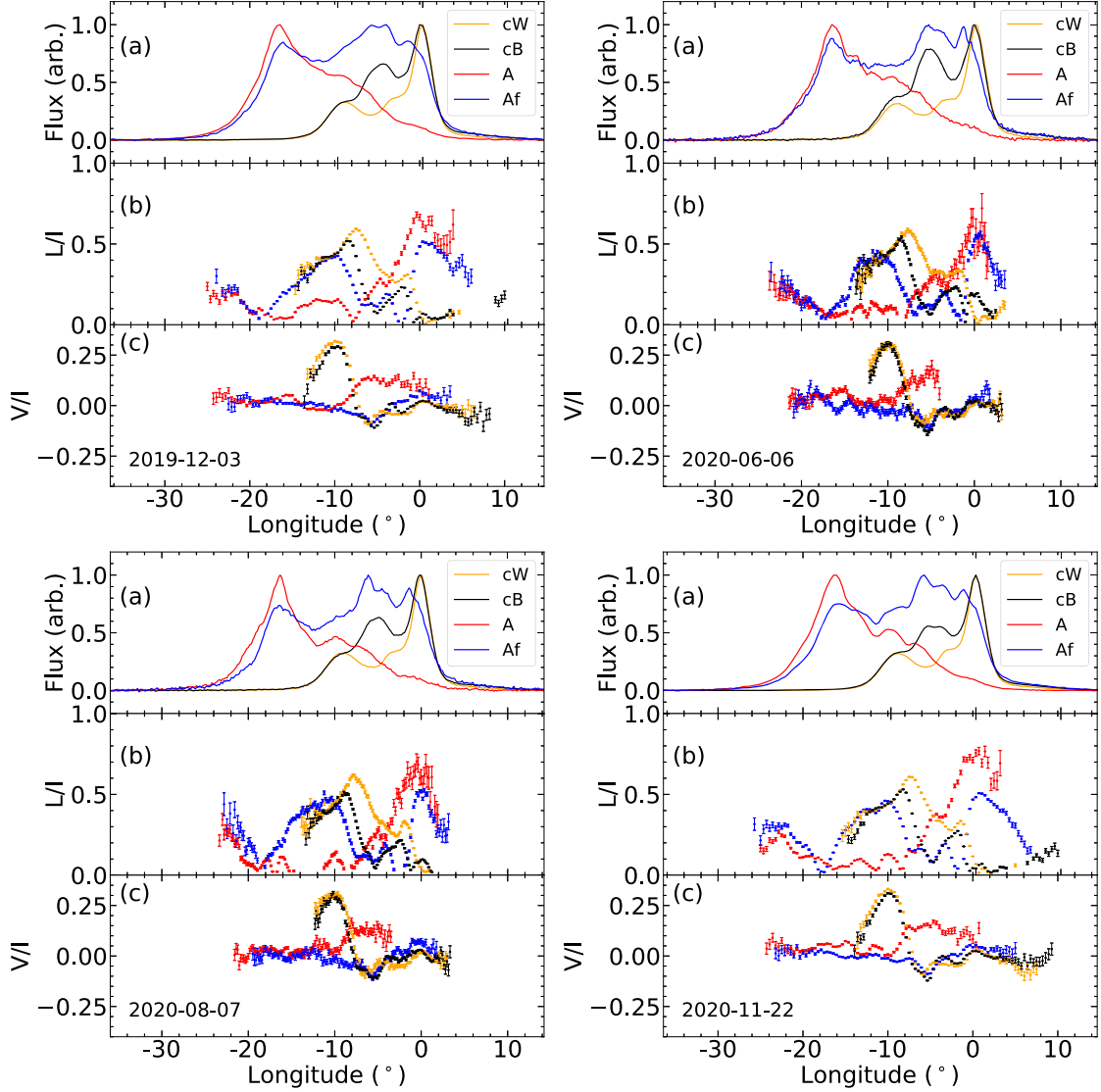


**Figure 4.** Comparison of mean pulse polarization profiles for the four modes (cW, cB, A and Af) obtained from four FAST observation sessions. The total intensity, fractional linear polarization and circular polarization are plotted in the different subpanels from top to bottom. The fractional linear polarization data are plotted only when linear polarization intensity exceeds five times the standard deviation of off-pulse data, and similarly for the fractional circular polarization.

much lower percentage in the phase range from  $-15^\circ$  to  $-7^\circ$ . For the emission of the Af mode, the fractional linear polarization is much higher at the leading and trailing parts of the profiles, but it is lower in the phase range from  $-8^\circ$  to  $-5^\circ$ . The very different fractional circular polarization is seen in the phase range from  $-14^\circ$  to  $-5^\circ$ . The normal modes have a sense-reversal at around  $-8^\circ$ , while the mode A has a peak in circular polarization at the phase of  $-5^\circ$  but the mode Af has a dip. In the other longitude ranges the circular polarization remains the same, and the circular polarization of the Af mode obviously follows the curve for the leading components of the A mode and the trailing components of the cW and cB modes.

All these polarization features suggest that the Af mode is a good “combination” of the “swooshes” of emission and two normal emission modes, indicating that the A mode is not the swooshed normal emission mode.

### 3.3. Subpulse Drifting in the Leading Component of the Af Mode

One, and only one, subpulse drifting event is identified from the leading component in the Af mode, as shown in Figure 5.

We fit the emission peaks in the phase range from  $-20^\circ$  to  $-12^\circ$  in these periods of the Af mode, and we find the drifting rate to be  $P_2/P_3 = -2.3$  per period. The period gap for a subpulse

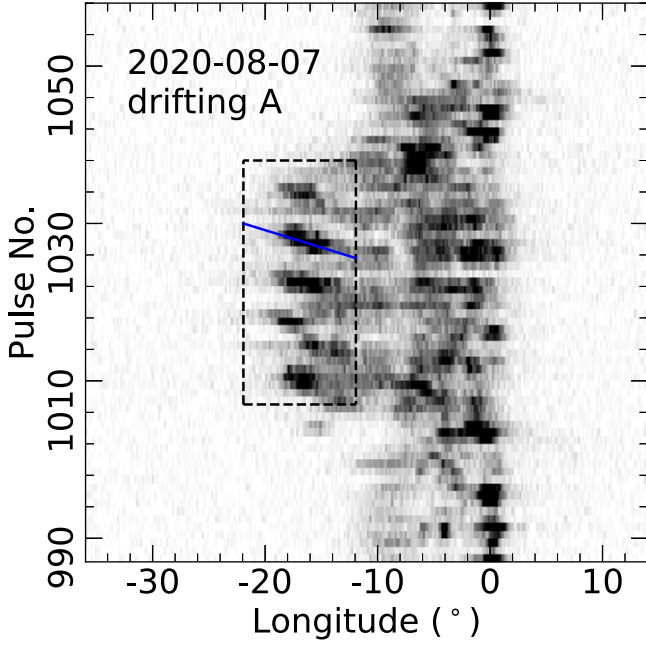


**Figure 5.** Subpulse drifting of PSR B1859+07 in the Af mode. The blue line indicates the direction of drift.

appearing at the same longitude, i.e.  $P_3$ , is measured to be six periods. The longitude spacing between two adjacent subpulses,  $P_2$ , derived from the cross-points of two drifting bands in a given period, is found to be  $-13^\circ 8$ .

#### 4. Summary and Discussion

In summary, based on the new FAST observations of PSR B1859+07, we find the following features for different modes.

(1) A new emission mode. We identify the Af mode, which is different from the previously known “swooshes” and has all components from the normal emission mode and anomalous “swooshes” which means that the emission components of the Af mode are not the swooshed components of normal emission, so that all such related theoretical interpretations involving “swoosh” should be abandoned.

(2) The duration of the anomalous emission modes. That should vary from a single rotation period to a few tens, as seen in Table 1.

(3) Emission phase ranges. Because the newly identified Af mode shows a much wide phase range for the emission, with the PA curves connecting PAs of the leading component in the anomalous mode and the trailing component in the normal emission mode, the normal mode should then be only a part of the illuminated conal emission, as for the partial cone discussed by Lyne & Manchester (1988) and Rankin et al. (2006).

(4) Orthogonal modes. The polarization angles for the “Af mode” coincide with the orthogonal mode of the “A mode” in some phase range, implying that they experience different propagation effects.

(5) Circular polarization. The circular polarization of normal mode emission changes the sense around the phase of  $-8^\circ$ , supporting the explanation of the normal emission profile as the partially illuminated conal emission (Rajwade et al. 2021).

(6) Subpulse drifting. We get the first detection of drifting subpulses for this pulsar in the leading component of the Af mode, and derive the drifting parameters from one drifting session. More data are desired for further investigation.

There have been a number of interpretations of the anomalous mode of PSRs B0919+06 and B1859+07. The models based on the aberration effects and the binary interactions have already been excluded by Rankin et al. (2006) and Wang et al. (2022). The polarization features of the newly identified mode of PSR B1859+07 favor the simple model in which the anomalous emission events are not caused by the so-called phase shift, but just the intrinsic radiation of different parts of the pulsar emission beam. The orthogonal mode between the different modes suggests possible changes in the energy and density distributions of relativistic particles for propagation effects in the entire pulsar magnetosphere (Wang et al. 2014). Since partial cones have been observed for many pulsars already (Lyne & Manchester 1988), which depends on sight-line geometry, the relativistic particles, various emission processes, and propagation effects, probably caused by dynamical sparking in the pulsar polar cap. The subpulse drifting occasionally observed and the sense-change of circular polarization are also key observational facts for understanding the anomalous mode of these pulsars.




#### Acknowledgments

FAST is a Chinese national mega-science facility built and operated by the National Astronomical Observatories, Chinese Academy of Sciences. P. F. Wang is supported by the National Key R&D Program of China (Nos. 2021YFA1600401 and 2021YFA1600400) and National Natural Science Foundation of China (Nos. 11873058 and 12133004). J. L. Han is supported by the National Natural Science Foundation of China (Nos. 11988101 and 11833009).

#### Data Availability

Original FAST observation data are accessible under the FAST data open policy, i.e., fully available one year after observations. All processed data as plotted in this paper can be obtained from the authors with a kind request.

### ORCID iDs

Tao Wang  <https://orcid.org/0000-0002-4704-5340>  
 P. F. Wang  <https://orcid.org/0000-0002-6437-0487>  
 J. L. Han  <https://orcid.org/0000-0002-9274-3092>

### References

- Bartel, N., Kardashev, N. S., Kuzmin, A. D., et al. 1981, *A&A*, **93**, 85  
 Gong, B. P., Li, Y. P., Yuan, J. P., et al. 2018, *ApJ*, **855**, 35  
 Han, J., Han, J. L., Peng, L.-X., et al. 2016, *MNRAS*, **456**, 3413  
 Han, J. L., Wang, C., Wang, P. F., et al. 2021, *RAA*, **21**, 107  
 Hotan, A. W., van Straten, W., & Manchester, R. N. 2004, *PASA*, **21**, 302  
 Jiang, P., Tang, N.-Y., Hou, L.-G., et al. 2020, *RAA*, **20**, 064  
 Lyne, A. G., & Manchester, R. N. 1988, *MNRAS*, **234**, 477  
 Nan, R. 2006, *Science in China: Physics, Mechanics and Astronomy*, **49**, 129  
 Nan, R., Li, D., Jin, C. J., et al. 2011, *IJMPD*, **20**, 989  
 Perera, B. B. P., Stappers, B. W., Weltevrede, P., Lyne, A. G., & Rankin, J. M. 2016, *MNRAS*, **455**, 1071  
 Rajwade, K. M., Perera, B. B. P., Stappers, B. W., et al. 2021, *MNRAS*, **506**, 5836  
 Rankin, J. M., Rodriguez, C., & Wright, G. A. E. 2006, *MNRAS*, **370**, 673  
 van Straten, W., & Bailes, M. 2011, *PASA*, **28**, 1  
 Wahl, H. M., Orfeo, D. J., Rankin, J. M., & Weisberg, J. M. 2016, *MNRAS*, **461**, 3740  
 Wang, L., Yu, Y.-Z., Kou, F., et al. 2022, *RAA*, **22**, 045001  
 Wang, P. F., Han, J. L., Xu, J., et al. 2023, *RAA*, **23**, submitted  
 Wang, P. F., Wang, C., & Han, J. L. 2014, *MNRAS*, **441**, 1943